Cancer Research

Cetuximab Resistance in Head and Neck Cancer Is Mediated by EGFR-K_{521} Polymorphism

Friederike Braig[1], Malte Kriegs[2], Minna Voigtlaender[1], Beate Habel[3], Tobias Grob[4], Karina Biskup[5], Veronique Blanchard[5], Markus Sack[6], Anja Thalhammer[7], Isabel Ben Batalla[1,8], Ingke Braren[9], Simon Laban[10], Antje Danielczyk[3], Steffen Goletz[3], Elzbieta Jakubowicz[11], Bruno Märkl[11], Martin Trepel[1,12], Rainald Knecht[13], Kristoffer Riecken[14], Boris Fehse[14], Sonja Loges[1,8], Carsten Bokemeyer[1], and Mascha Binder[1]

Abstract

Head and neck squamous cell carcinomas (HNSCC) exhibiting resistance to the EGFR-targeting drug cetuximab poses a challenge to their effective clinical management. Here, we report a specific mechanism of resistance in this setting based upon the presence of a single nucleotide polymorphism encoding EGFR-K_{521} (K-allele), which is expressed in >40% of HNSCC cases. Patients expressing the K-allele showed significantly shorter progression-free survival upon palliative treatment with cetuximab plus chemotherapy or radiation. In several EGFR-mediated cancer models, cetuximab failed to inhibit downstream signaling or to kill cells harboring a high K-allele frequency. Cetuximab affinity for EGFR-K_{521} was reduced slightly, but ligand-mediated EGFR activation was intact. We found a lack of glycan sialyation on EGFR-K_{521} that associated with reduced protein stability, suggesting a structural basis for reduced cetuximab efficacy. CetuGEX, an antibody with optimized Fc glycosylation targeting the same epitope as cetuximab, restored HNSCC sensitivity in a manner associated with antibody-dependent cellular cytotoxicity rather than EGFR pathway inhibition. Overall, our results highlight EGFR-K_{521} expression as a key mechanism of cetuximab resistance to evaluate prospectively as a predictive biomarker in HNSCC patients. Further, they offer a preclinical rationale for the use of ADCC-optimized antibodies to treat tumors harboring this EGFR isoform. *Cancer Res; 77(5); 1188–99. ©2016 AACR.*

Introduction

Head and neck squamous cell carcinomas (HNSCC) are among the most common types of newly diagnosed cancers in men with disappointing outcomes despite intensive treatment (1–8). Cetuximab, a mAb targeting the extracellular ligand-binding domain of the EGFR, has been shown to prolong overall survival in patients with recurrent or metastatic disease by about three months compared with chemotherapy alone. It has therefore been approved in combination with platinum-based chemotherapy (EXTREME protocol; ref. 7). Treatment efficacy of cetuximab, however, is low with an objective response rate of 13% in the monotherapy setting (9) and 36% in combination with chemotherapy (7). Time-to-treatment failure in patients treated with the EXTREME regimen ranges only around 5 months despite cetuximab maintenance (7).

Together, this suggests that primary and acquired resistance mechanisms considerably limit the clinical benefit of cetuximab in HNSCC. There is, therefore, a clear need to understand the molecular mechanisms ultimately driving cetuximab resistance to maximize the likelihood of response by biomarker-driven patient selection and to establish new treatment options to overcome resistance. In this context, a number of potential resistance-mediating molecular alterations and pathways have been studied in HNSCC. Whereas activating mutations of the *Rat* sarcoma genes (KRAS and NRAS) downstream of the GFR constitute an important mechanism of primary

[1]Department of Oncology and Hematology, BMT with Section Pneumology, University Medical Center Hamburg-Eppendorf, Hamburg, Germany. [2]Radiation Biology and Radiooncology, University Medical Center Hamburg-Eppendorf, Hamburg, Germany. [3]Bioassays and Nonclinical Studies, GLYCOTOPE GmbH, Berlin, Germany. [4]Department of Pathology, University Medical Center Hamburg-Eppendorf, Hamburg, Germany. [5]Institute for Laboratory Medicine, Clinical Chemistry and Pathobiochemistry, Charité University Medical Center Berlin, Berlin, Germany. [6]Fraunhofer Institute for Molecular Biology and Applied Ecology IME, Aachen, Germany. [7]Department of Physical Biochemistry, Potsdam University, Potsdam, Germany. [8]Institute for Tumor Biology, University Medical Center Hamburg-Eppendorf, Hamburg, Germany. [9]HEXT Vector Facility/Institute for Experimental Pharmacology and Toxicology, University Medical Center Hamburg-Eppendorf, Hamburg, Germany. [10]Department of Oto-Rhino-Laryngology and Head and Neck Surgery, Ulm University Medical Center, Ulm, Germany. [11]Pathological Institute, Klinikum Augsburg, Augsburg, Germany. [12]Department of Oncology and Hematology, Klinikum Augsburg, Augsburg, Germany. [13]Department of Otorhinolaryngology, Head and Neck Cancer Center of the University Cancer Center Hamburg, University Medical Center Hamburg, Hamburg, Germany. [14]Research Department Cell and Gene Therapy, Department of Stem Cell Transplantation, University Medical Center Hamburg-Eppendorf, Hamburg, Germany.

Note: Supplementary data for this article are available at Cancer Research Online (http://cancerres.aacrjournals.org/).

Corresponding Author: Mascha Binder, University Medical Center Hamburg-EppendorfHubertus Wald Cancer Center, Martinistrasse 52, Hamburg D-20246, Germany. Phone: 4940-7410-58787; Fax: 4940-7410-40555; E-mail: m.binder@uke.de

doi: 10.1158/0008-5472.CAN-16-0754

resistance to EGFR-targeting antibodies in colorectal cancer (10–12), these proto-oncogenes are virtually never expressed at baseline in HNSCC and, therefore, cannot be used as predictive biomarker for patient selection (13). Other potential biomarkers such as EGFR expression level (14), alterations of the EGFR itself [e.g., EGFR polymorphisms, EGFR variant III (vIII) expression (15, 16), nuclear EGFR, arginine methylation within the extracellular EGFR domain (17)], alternative tyrosine kinase signaling (e.g., ErbB signaling, MET activation, Axl overexpression; ref. 18), or alterations in targets downstream the EGFR (e.g., activating HRAS mutations, loss of PTEN, deregulated PI3K pathway; refs. 19, 20) have been evaluated. Yet, none of these alterations are sufficiently understood in HNSCC and prospective trials confirming their clinical utility are lacking (13, 16, 21, 22). Therefore, to date, there is not a single predictive biomarker allowing patient selection for EGFR-directed therapy in HNSCC (23).

Here, we studied a genomic SNP within exon 13 of the extracellular receptor domain ($EGFR_{K521}$) that is homo- or heterozygously expressed in >40% of individuals and has previously been reported to be associated with impaired response to cetuximab in small clinical HNSCC series (22, 24, 25). We confirm these clinical data in our own cohort of 59 HNSCC patients as well as in two *in vitro* models and in a mouse xenograft model. Our molecular data propose that differential posttranslational modifications may represent the structural basis for the inability of cetuximab to block signal transduction in this receptor variant. We then go on to show how this resistance may be overcome by using next-generation EGFR antibodies mainly relying on optimized recruitment of effector cells for killing. This work suggests that $EGFR_{K521}$ expression represents an important mechanism of primary resistance to cetuximab in HNSCC and may be used as a biomarker to select patients for treatment with cetuximab. Furthermore, we provide a strong preclinical rationale for the use of alternative EGFR-targeting antibodies in this subset of patients. Both the biomarker aspect of our data and potential ways of alternative EGFR targeting warrants validation in prospective clinical trials translating these findings into therapeutic refinements in our regimens to ultimately improve our care for patients with HNSCC.

Materials and Methods

Patient characteristics

The Clinical Cancer Registry of the University Cancer Center Hamburg and Augsburg Medical Center was screened for HNSCC patients treated in a palliative setting between 2010 and 2016 (Augsburg: 2011–2016). All patients were screened for HPV status and were excluded, if they were positive for both HPV-DNA and p16 IHC. Patient characteristics are shown in Supplementary Table S1.

Cell lines

HNSCC cell lines were cultivated in DMEM (Life Technologies) and identified using a short tandem repeat multiplex assay (Life Technologies). UT-SCC cell lines 5, 8, 14, 15, 29, 42A, and 60A were kindly provided by R. Grenman in 2011 (University of Turku, Turku, Finland), FaDuDD by W. Eicheler (University of Dresden, Dresden, Germany; ref. 17) and Cal 33, HSC 4, SAS, SAT by M. Baumann in 2006 (University of Dresden, Dresden, Germany). Ba/F3 cells (CSC-C2045, Creative Bioarray) were maintained in RPMI (Life Technologies) containing 10 ng/mL murine IL3 (PeproTech). KHYG1 cells were purchased (DSMZ) and maintained in RPMI containing 10 ng/mL IL2 (PeproTech). KHYG1 cells were stably transfected with human FcγRIIIa 158F (KHYG1-CD16aF), cloned, and maintained in medium containing 25 nmol/L methotrexate (Sigma-Aldrich). All cell lines were mycoplasma-free (VenorGeM kit, Merck Millipore). Ba/F3 and KHYG1 cells were obtained in 2009 and 2012, respectively.

Determination of $EGFR_{K521}$ status in HNSCC cell lines and tumor tissue

$EGFR_{K521}$ status determination was performed from genomic DNA (gDNA) extracted from tumor material with >80% infiltration or cell lines using the GenElute Mammalian Genomic DNA Miniprep Kit (Sigma-Aldrich) by EGFR exon 13 next-generation sequencing as described previously (26). Fifty percent was used as a cutoff separating cell lines with low and high K-allele frequency. Patient tumors were classified as homo- or heterozygous for the K-allele based on >0% K-allele detection by NGS.

HNSCC cell line cetuximab inhibition assays and *EGFR/pEGFR* determination

Cell survival was measured by colony formation after treatment with 5 μg/mL cetuximab (clone number: C225, Erbitux, Merck Serono GmbH). Twenty-four hours later, cells were replated, colonies fixed with 70% ethanol for 5 minutes, stained with crystal violet (Merck Millipore). Colonies of more than 50 cells were scored as "survivors."

Cell lysates taken after two hours or at indicated time points were analyzed by Western blot analysis as described previously (26). Primary antibodies used were anti-EGFR (catalog number: 2232) and anti-pEGFR (pTyr1173; clone number: 53A5, Cell Signaling Technology). Secondary antibodies used were IRDye 680RD–labeled anti-mouse (catalog number: 926-68070) and IRDye 800CW labeled anti-rabbit antibodies (catalog number: 926-32211, LI-COR Biosciences). Membrane EGFR was quantified by flow cytometry using the Quantum Simply kit (Bangs Laboratories, Inc.).

EGFR/$EGFR_{K521}$ transduced Ba/F3 stimulation and inhibition experiments

The cDNA sequence of the *EGFR* was cloned into the lentiviral vector LeGO-iG3 (26), containing a modified multiple cloning site, resulting in LeGO-iG3-EGFR (eGFP). The $EGFR_{K521}$ insert was generated using the QuikChange XL Site-Directed Mutagenesis Kit (Agilent Technologies). Virus production and transduction was described earlier (27). Cells with a transduction rate of 25% and thus containing mostly single integrations were sorted (FACSAria). Ligand stimulation of *EGFR*/$EGFR_{K521}$–transduced Ba/F3–sorted sublines was performed by switching cells from IL3 to medium containing 5 ng/mL of either EGF, HB-EGF, betacellulin, epigen, epiregulin, amphiregulin or TGF (PeproTech). Cells were counted (Vi-CELL Cell Viability Analyzer, Beckman Coulter) and ligand or inhibitor added every 24 hours.

HNSCC *EGFR*/$EGFR_{K521}$–expressing xenograft mouse model

Six- to 8-week-old female NSG (NOD.Cg-Prkdcscid Il2rgtm1Wjl/SzJ) mice were purchased from The Jackson Laboratory. Experiments were performed under a 12-hour light–dark

cycle and standard laboratory conditions. For the xenograft models, 1×10^7 UT-SCC 42A or SAS cells were injected subcutaneously into the right flank. Mice were randomized for tumor size after 7–9 days (mean tumor size 80–150 mm^3) and treated with 1 mg of cetuximab intraperitoneally twice weekly. Tumor volume was calculated [$V = (\text{longer length}^2 \times \text{shorter length})/2$] and mice were sacrificed due to ethical regulations when the first tumor in the control group reached 1,500 mm^3.

Cetuximab binding to HNSCC cell lines and *EGFR*-transduced Ba/F3 cells

HNSCC cell lines UT-SCC 8, SAT, and *EGFR*/$EGFR_{K521}$–transduced Ba/F3 cells were stained with the following antibodies: polyclonal goat-anti-EGFR antibody (catalog number: AF231, R&D Systems), polyclonal goat-anti-human kappa (catalog number: 2060-01, Southern Biotech), cetuximab, rituximab (clone number: 10F381, MabThera, Roche Diagnostics), anti-goat IgG-APC (catalog number: F0108, R&D Systems), and anti-Human Ig, κ Light Chain-APC (clone number: G20-193, Becton Dickinson). Cells were analyzed on a FACSCalibur (Becton Dickinson).

Expression of EGFR-Fc fusion proteins

cDNAs coding for the human *EGFR*/$EGFR_{K521}$ ectodomain (aa 1–645) and the human *IgG1* Fc fragment were cloned into LeGO-iG3-Puro+ (28). Virally transduced and puromycin-selected HEK293T cells (CRL-11288, ATCC) were used to produce Fc-EGFR fusion proteins purified from conditioned medium by an anti-EGFR scFv (cloned in *pKB2scFvCBD* and expressed as described by Blank and colleagues; ref. 29) attached to a chitin resin (New England Biolabs).

Affinity studies of Fc-EGFR fusion proteins

Plasmon resonance analysis was performed on a BIAcore T200 (GE Healthcare). EGFR-Fc fusion proteins were captured directly from the supernatant by immobilized protein A. The capture levels were adjusted for the different EGFR-Fc preparations to obtain maximum saturation responses (R_{max}) for the Fab of cetuximab of $R_{max} = 25$-50RU. The Fab was prepared by proteolytic digestion of cetuximab using Pierce Fab Preparation Kit (Thermo Scientific) followed by negative protein A affinity purification. Double referenced binding curves were fitted to a simple monovalent interaction model.

Analysis of $EGFR_{K521}$-associated post-translational modifications

Fc-EGFR/Fc-$EGFR_{K521}$ fusion proteins were digested with α2-3,6,8,9 Neuraminidase A (New England Biolabs). Two-dimensional (2D) gel electrophoresis of digested and undigested Fc-EGFR/Fc-$EGFR_{K521}$ was performed using Immobiline DryStrip pH 3-10NL (GE Healthcare) and polyacrylamide gels, followed by Coomassie staining and spot excision for MALDI-TOF-MS glycosylation analysis. Gel pieces were destained, dried, and redissolved in phosphate buffer containing N-octyl-β-glucopyranoside (OGP; 8 mg/mL) and subjected to PNGase F digestion (Roche Applied Science). *N*-glycans were extracted from gel pieces with acetonitrile, dried, desalted, and permethylated as described previously (30). MALDI-TOF mass spectra were recorded on an Ultraflex III mass spectrometer (Bruker Daltonics).

Fc-EGFR fusion protein stability analysis by far-UV circular dichroism spectroscopy

Far-UV circular dichroism (CD) spectra of 0.2 g/L Fc-EGFR/Fc-$EGFR_{K521}$ in 0.01 mol/L PBS at 23°C were recorded using a 1-mm path length cuvette in a Jasco-815 spectropolarimeter (Jasco Instruments). Melting curves were recorded at a fixed wavelength of 208 nm over a temperature range from 23°C to 100°C. Data were transformed to mean residue ellipticity [θ] after subtraction of the buffer signal.

Antibody-dependent cellular cytotoxicity analyses

The antibody-dependent cellular cytotoxicity (ADCC) assay was performed as europium release assay using either *EGFR*-positive HNSCC cell lines or *EGFR*-transduced Ba/F3 cells as target cells and a NK cell line stably transfected with human *FcγRIIIa 158F* (KHYG1-CD16aF) as effector cells. Briefly, target cells were loaded with europium by electroporation (Nucleofector) and incubated with a dilution series of CetuGEX (clone number: P142-C5, Glycotope Biotechnology GmbH) or cetuximab and KHYG1-CD16aF (effector-to-target ratio, 10:1) for 5 hours. Europium release was quantified by time-resolved fluorescence (Infinite F200, Tecan Austria GmbH). Maximum release (MR) was measured after incubation of target cells with triton X-100 (Sigma-Aldrich) and spontaneous release (SR) was obtained from samples containing only target cells. Basal release (BR) was determined in target cell supernatant collected directly after europium loading. Spontaneous lysis in percent was calculated as the percentage of SR to MR corrected for the observed BR [$(SR - BR) \times 100/(MR - BR)$]. Specific cytotoxicity (% specific lysis) was calculated as the percentage of experimental release (ER) to MR corrected for the observed SR [$(ER - SR) \times 100/(MR - SR)$]. Specific lysis versus antibody concentration curves were fitted using a 4 parameter logistic function.

Statistical analysis

Survival was analyzed with Kaplan–Meier method and Breslow test (Generalized Wilcoxon) using SPSS. Data represent mean ± SEM of three representative experiments, unless otherwise stated. Statistical significance was calculated by Student *t* test unless otherwise stated.

Study approval

Patient informed consent was obtained for the use of their diagnostic material as approved by the institutional review board (project number PV4382: Hamburg; no number assigned: Augsburg).

All animal experiments were carried out according to the institutional guidelines for the welfare of animals in experimental neoplasia as approved by the local licensing authority (project number G126/15).

Results

$EGFR_{K521}$ status correlates with shorter progression-free survival in HNSCC patients undergoing cetuximab-based treatment

The SNP *$EGFR_{K521}$* is located outside the cetuximab epitope on the opposite face of receptor domain III (Fig. 1). Here, we determined the *$EGFR_{K521}$* status in 59 HPV-negative HNSCC patients receiving cetuximab in a palliative situation, either in

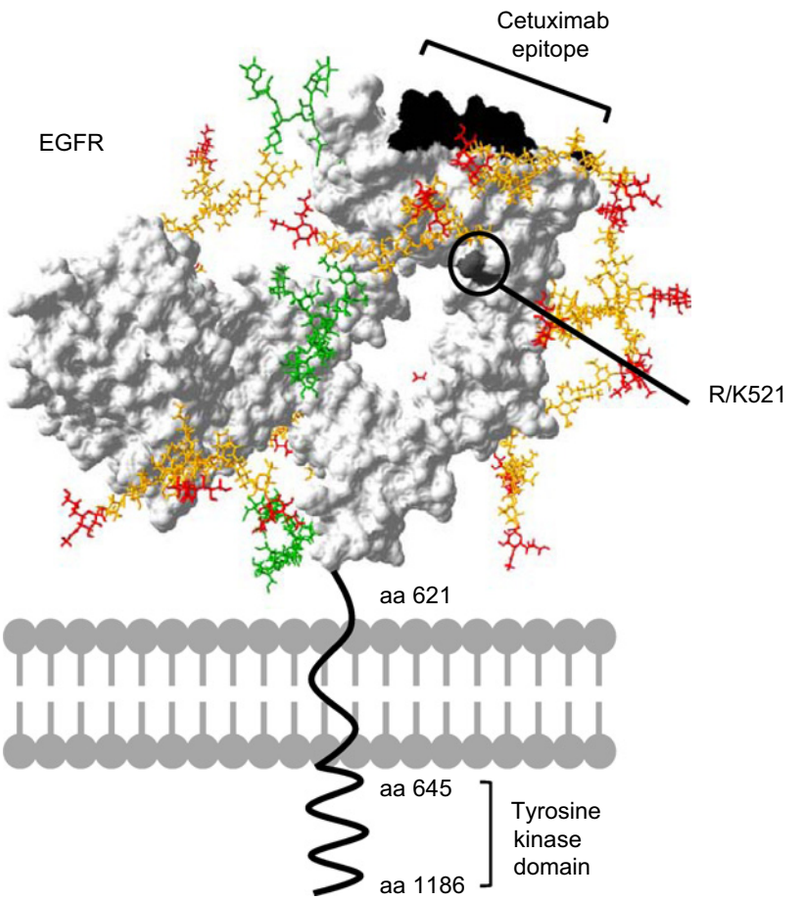

Figure 1.
Structural illustration of the EGFR showing the cetuximab epitope and the SNP at position 521. The 3D model created from pdb file 1YY9 (RCSB Protein Data Bank) includes *N*-glycans of the oligomannose-type (green) and complex-type (orange) with terminal sialic acids (red). *N*-glycans were integrated as published previously (31).

combination with chemotherapy or with radiation. Patient characteristics are displayed in Supplementary Table S1. Thirty-three of 59 patients (55.9%) were homo- or heterozygous for the K-allele (Supplementary Table S1). These showed significantly shorter progression-free survival (median 4.93 months; 95% CI, 3.52–6.34) than patients not expressing the K-allele (median 8.25 months; 95% CI, 3.25–13.26; $P = 0.049$; Fig. 2). Despite not being powered for overall survival analysis, these data confirm previous studies suggesting a poor response to cetuximab in HNSCC patients expressing $EGFR_{K521}$ (22, 24).

Cetuximab fails to inhibit HNSCC cell lines with a high K-allele frequency *in vitro*

Next, we determined $EGFR_{K521}$ status in 12 HNSCC cell lines by next-generation sequencing. Fifty-percent of these showed low (UT-SCC 42A, UT-SCC 8, UT-SCC 14, UT-SCC 29, Cal 33, UT-SCC 15) and high (SAS, UT-SCC 5, UT-SCC 60A, FaDuDD, HSC 4, SAT) K-allele frequencies (cut-off 50%), respectively. We treated these lines for 24 hours with cetuximab followed by replating. In cell lines with a high frequency of K-alleles, colony formation was not significantly inhibited as compared with the untreated control and in contrast to cell lines with low K-allele frequency, suggesting insensitivity to cetuximab under *in vitro* conditions (Fig. 3A). Colony formation was equally suppressed, however, in all cell lines treated with erlotinib, generally indicating cellular dependency on the EGFR pathway (Fig. 3A). Cell lines with high K-allele frequency did not show significant inhibition of EGFR phosphorylation upon cetuximab treatment for 2 hours compared with cells with lower K-allele frequency, while erlotinib inhibited phosphorylation

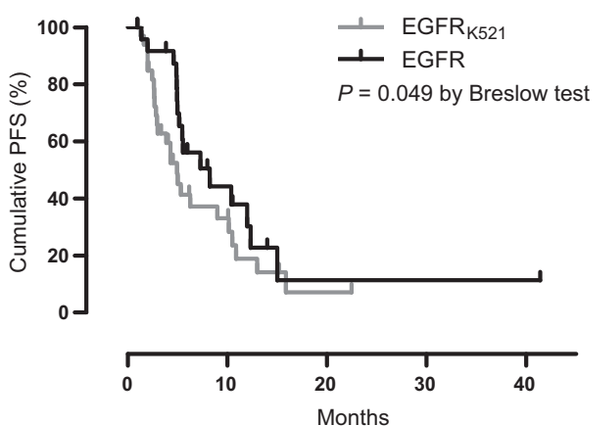

Figure 2.
Progression-free survival (PFS) in cetuximab-treated HNSCC patients with or without $EGFR_{K521}$ expression. Fifty-nine HPV-negative HNSCC patients received palliative cetuximab treatment in combination with chemotherapy or with radiation. The Kaplan–Meier method including Breslow test was used to compare progression-free survival in patients with or without expression of $EGFR_{K521}$.

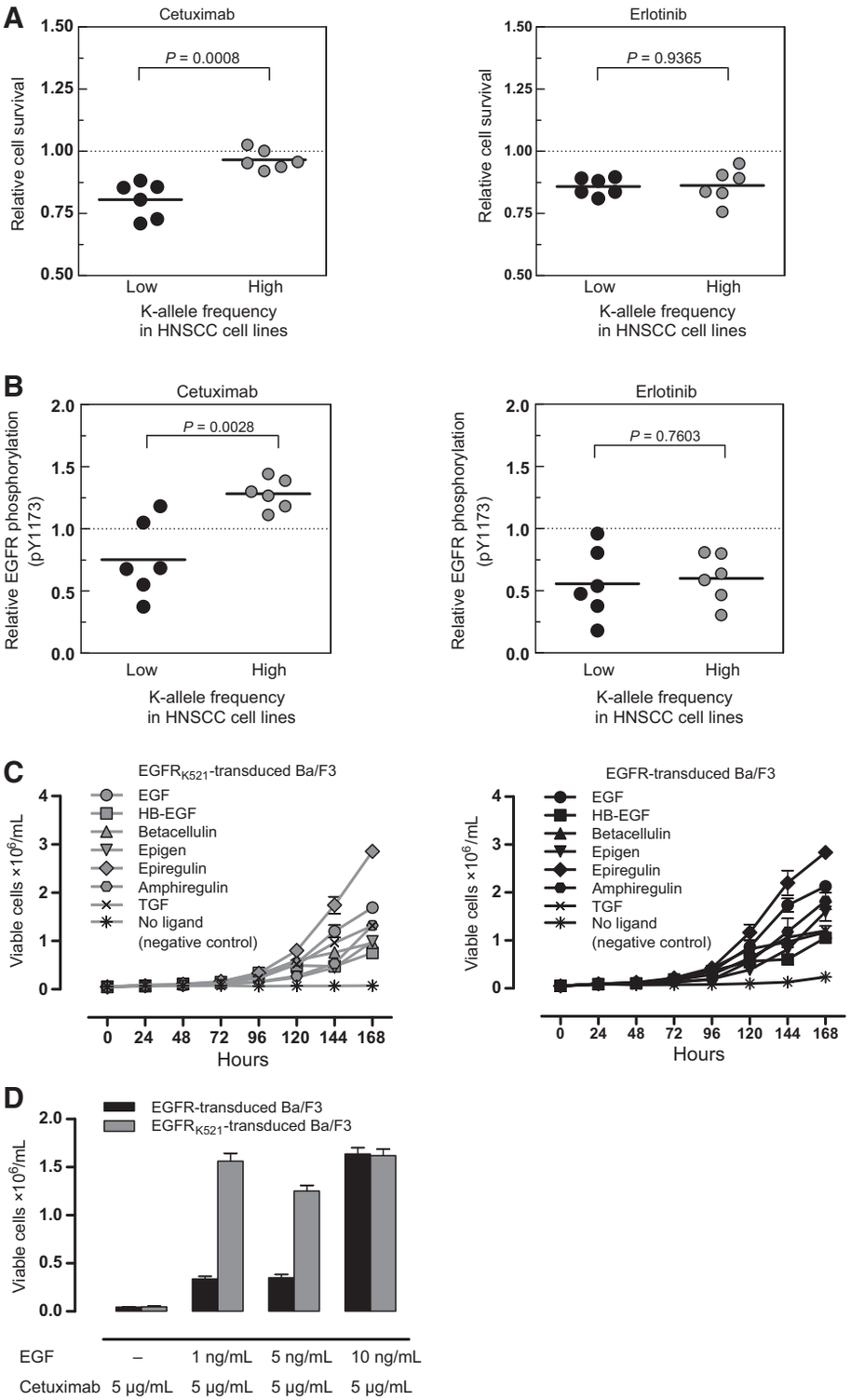

Figure 3.

In vitro inhibition of EGFR$_{K521}$-expressing cell lines by cetuximab. **A** and **B,** Inhibition of colony formation (**A**) and EGFR phosphorylation (**B**) by cetuximab or erlotinib in a set of HNSCC cell lines with high or low K-allele frequencies. Data are shown as relative values compared with untreated cells. **C,** Functionality of EGFR and EGFR$_{K521}$ variants in neutral Ba/F3 cellular background. Proliferation was measured by counting of viable cells in the absence or presence of multiple EGFR ligands. **D,** Effect of cetuximab on EGFR versus EGFR$_{K521}$-transduced Ba/F3 cells. Cells were cultured for 96 hours with 5 µg/mL cetuximab and increasing EGF concentrations. *, $P < 0.05$; ***, $P < 0.001$ by Student *t* test. n.s., not significant.

in both sets of cell lines (Supplementary Fig. S1; Fig. 3B). Some cell lines did not show inhibited EGFR phosphorylation at this time point despite effects on colony formation, but time course experiments confirmed inhibited phosphorylation at an earlier time point as shown for UT-SCC 8 in Supplementary Fig. S2. Quantification of total EGFR (by Western blot analysis) and membrane-exposed EGFR (by determination of antibody-binding capacity) demonstrated equal distribution in the two sets of

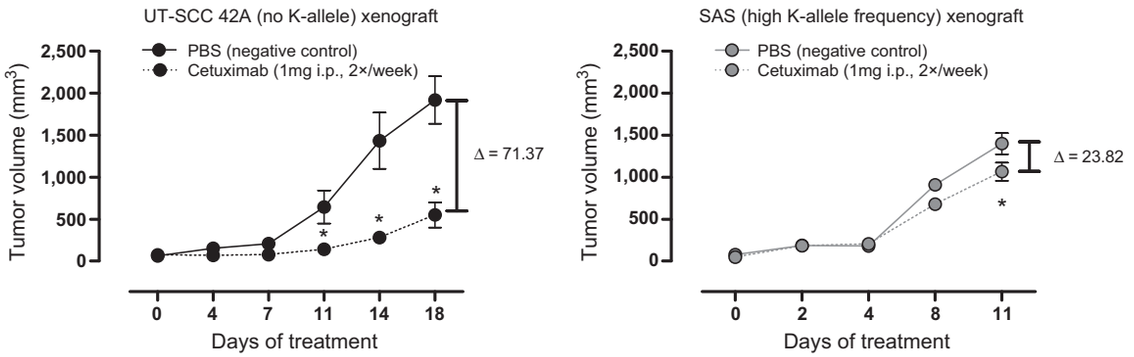

Figure 4.

In vivo Inhibition of HNSCC xenografts with or without $EGFR_{K521}$ expression by cetuximab. UT-SCC 42A (no K-allele) and SAS (high K-allele frequency) cells were injected subcutaneously in NOD-SCIDγ mice. Mice were treated with 1 mg (abs.) cetuximab or PBS (negative control) intraperitoneally twice per week, once tumors reached a size of 100 mm^3. *, $P < 0.05$ by Student *t* test.

cell lines, confirming that this factor is not a confounder in this analysis (Supplementary Fig. S3). Our findings strongly suggested that insensitivity to cetuximab directly relied on its inability to block the EGFR pathway in the $EGFR_{K521}$ receptor variant.

Cetuximab shows lack of $EGFR_{K521}$ inhibition in a neutral Ba/F3 cellular background *in vitro*

Next, we wished to confirm that this mechanism exclusively involved the EGFR itself and was not related to other mechanisms of resistance that may be correlated with the $EGFR_{K521}$ status. To this end, we analyzed cetuximab-mediated cell inhibition in a neutral cellular background of EGF-dependent EGFR- and $EGFR_{K521}$–expressing cells. Therefore, the IL3-dependent and EGFR-negative Ba/F3 cell line was lentivirally transduced with an expression vector encoding *EGFR* or $EGFR_{K521}$. Because of stable *EGFR* oncogene expression, these transduced cell lines could subsequently be rescued from IL3 withdrawal by EGF stimulation (Supplementary Fig. S4). To definitively confirm identical functional properties and susceptibility to ligand-mediated pathway activation in EGFR- and $EGFR_{K521}$-expressing cells, we stimulated the transduced Ba/F3 cell lines with a range of established EGFR ligands. These experiments showed identical proliferation in both cell lines, confirming intact receptor function of the $EGFR_{K521}$ variant (Fig. 3C). As expected, however, cetuximab exclusively showed inhibitory activity in EGFR-transduced cells (only blockable by excess concentrations of EGF), but not in $EGFR_{K521}$-transduced cells (Fig. 3D). These findings were in line with the differential killing effects observed in the two sets of HNSCC cell lines and once more demonstrated the insensitivity of $EGFR_{K521}$-expressing cells to cetuximab.

In vivo cetuximab treatment is ineffective in mice bearing $EGFR_{K521}$-expressing HNSCC xenografts

To confirm insensitivity of $EGFR_{K521}$-expressing HNSCC to cetuximab *in vivo*, we generated a xenograft mouse model using the cell lines UT-SCC 42A (no K-allele) and SAS (high K-allele frequency) exhibiting similar EGFR expression levels. Out of the HNSCC cell lines, this pair exhibited most comparable growth characteristics in the xenograft model and was therefore chosen for the *in vivo* experiments. Treatment with cetuximab was initiated after randomization when tumors reached a size of 100 mm^3 with twice-weekly dosing and mice were sacrificed when the first tumor reached a size of 1,500 mm^3. While UT-SCC 42A xenografts were significantly inhibited by cetuximab, SAS xenografts were virtually insensitive to this treatment. These results were in line with our *in vitro* data (Fig. 4).

Cetuximab affinity to $EGFR_{K521}$ is slightly reduced

Flow cytometric cetuximab-binding studies on cell lines expressing exclusively $EGFR_{K521}$ suggested that cetuximab binding to the receptor variant was preserved with mean fluorescence intensities comparable with EGFR-expressing cells (Fig. 5A). As (even minor) decreases in antibody affinity may entail considerable loss of pathway-inhibitory function even if cell attachment is preserved, we studied the affinity of cetuximab to $EGFR_{K521}$ on the protein level. Therefore, Fc fusion proteins encompassing the extracellular domains of $EGFR_{K521}$ and EGFR were recombinantly expressed in HEK293T cells and purified from the supernatant. Plasmon resonance–binding studies showed a very slight but significant reduction in cetuximab affinity to Fc-$EGFR_{K521}$ compared with Fc-EGFR (Fig. 5B).

$EGFR_{K521}$ shows nonsialylated high-mannose *N*-glycans at extracellular glycosylation sites

From a biochemical perspective, the $EGFR_{K521}$ variant *prima vista* involves an insignificant amino acid exchange (arginine to lysine). Moreover, the position itself does not harbor any known posttranslational modifications (31). We therefore broadly searched for global changes in posttranslational modifications within the receptor variant that could potentially explain the rather unexpected impact on the effect of cetuximab. To this end, Fc-$EGFR_{K521}$ and Fc-EGFR were analyzed by two-dimensional gel electrophoresis. Interestingly, protein species patterns were clearly different in these EGFR variants, despite exchange of only one (biochemically similar) amino acid (Fig. 6A, row one and three). While Fc-EGFR showed many protein species, scattered between pH 5 and 7, Fc-$EGFR_{K521}$ showed only protein species around pH 7. As posttranslational modifications of the extracellular EGFR domain are virtually restricted to N-glycosylation (Fig. 1) and as the molecular weight of the Fc-$EGFR_{K521}$ and Fc-EGFR fusion proteins appeared to be identical, we hypothesized that minor changes in glycosylation without effect on molecular

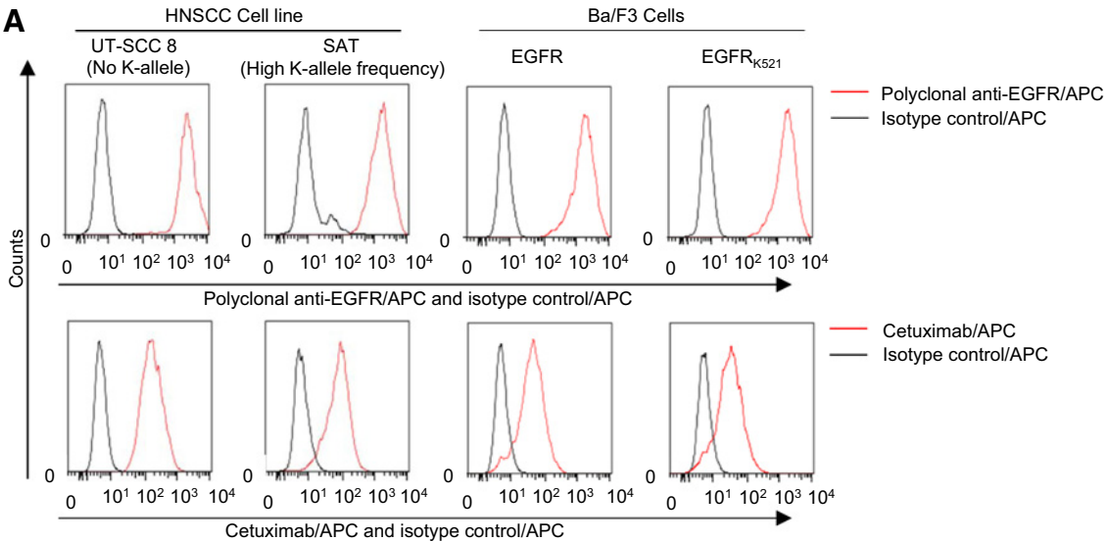

Cell line	Detection antibody	MFI
UT-SCC 8	Polyclonal anti-EGFR	2267
SAT	Polyclonal anti-EGFR	1512
EGFR-transduced Ba/F3 cells	Polyclonal anti-EGFR	1625
EGFR$_{K521}$-transduced Ba/F3 cells	Polyclonal anti-EGFR	1731
UT-SCC 8	Cetuximab	204
SAT	Cetuximab	79
EGFR-transduced Ba/F3 cells	Cetuximab	37
EGFR$_{K521}$-transduced Ba/F3 cells	Cetuximab	28

MFI, mean fluorescence intensity; **HNSCC,** head and neck squamous cell carcinoma; **APC,** allophycocyanin

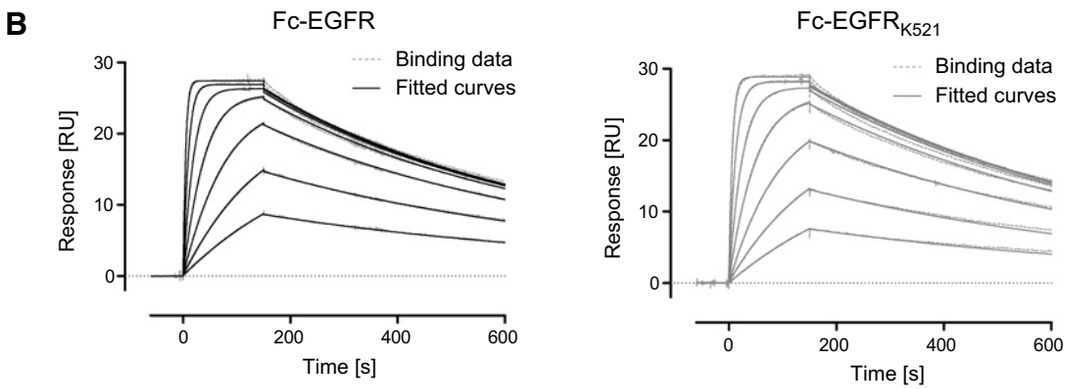

	K_{on} ($M^{-1}s^{-1}$)	K_{off} (s^{-1})	K_d (pmol/L)
Fc-EGFR	6.33×10^6	1.78×10^{-3}	282
Fc-EGFR$_{K521}$	4.24×10^6	1.60×10^{-3}	368

Figure 5.

Binding properties and affinity of cetuximab to EGFR$_{K521}$-expressing cell lines and Fc-EGFR$_{K521}$. **A,** Binding of cetuximab to EGFR$_{K521}$-expressing cells. HNSCC cell lines with no and high K-allele frequency and EGFR/EGFR$_{K521}$–transduced Ba/F3 cells were subjected to flow cytometry using cetuximab and polyclonal anti-EGFR as detection antibodies. Mean fluorescence intensity (MFI) values are shown. **B,** Analysis of cetuximab affinity to Fc-EGFR and Fc-EGFR$_{K521}$ recombinantly expressed fusion proteins by surface plasmon resonance. Binding data and fitted curves are shown as dotted and solid lines, respectively. Association rate (K_{on}), dissociation rate (K_{off}), and equilibrium binding constant (K_d) are shown.

weight, such as sialylation, could potentially explain the divergent protein species in Fc-EGFR$_{K521}$ and Fc-EGFR. To address the impact of sialylation, we specifically desialylated the Fc-EGFR and Fc-EGFR$_{K521}$ proteins with neuraminidase. As expected, the protein species of desialylated Fc-EGFR shifted toward pH 7 (Fig. 6A, second row), thus converging with the Fc-EGFR$_{K521}$

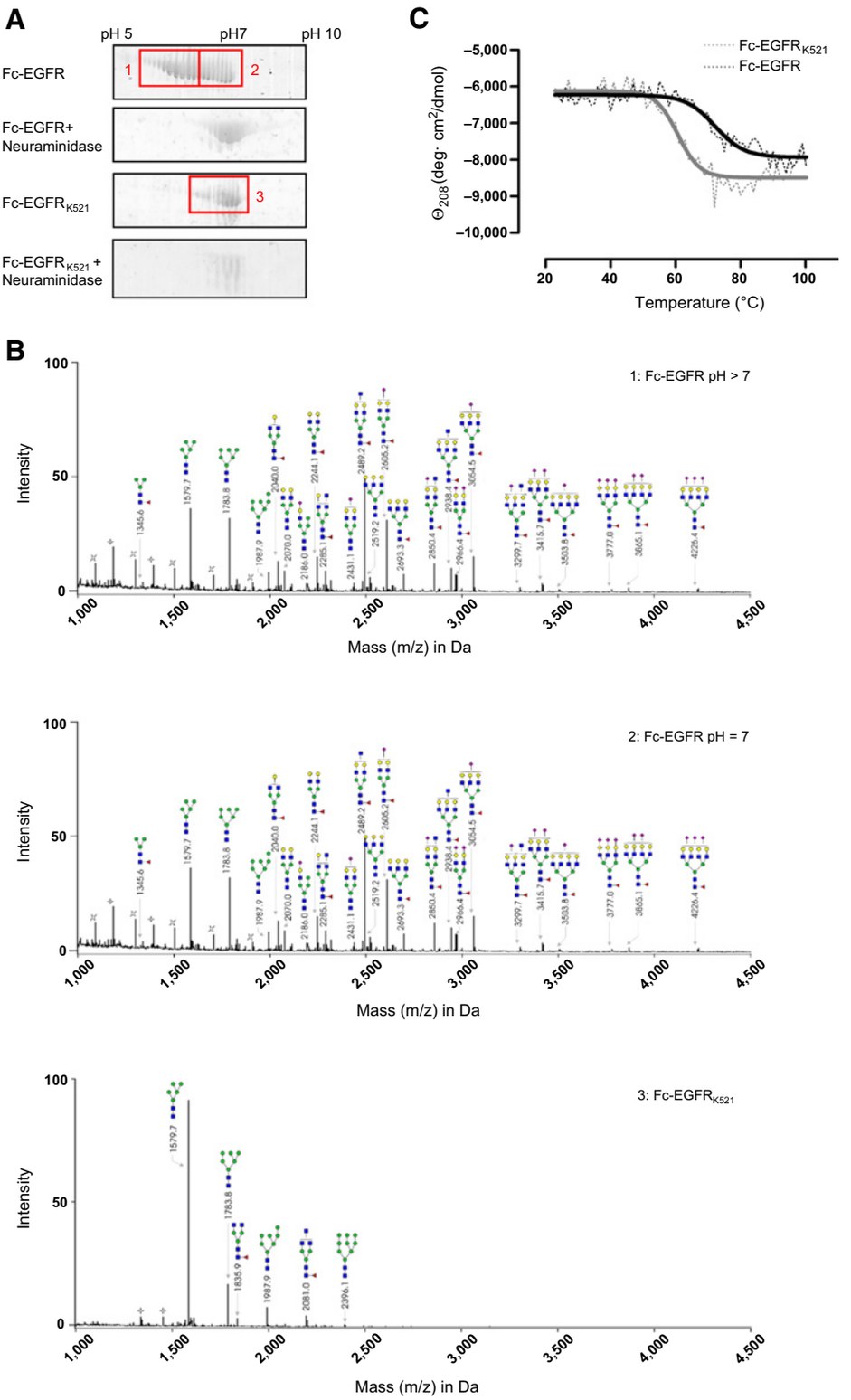

Figure 6.
Posttranslational modifications and stability of EGFR$_{K521}$. **A,** 2D separated and Coomassie-stained protein species of Fc-EGFR, Fc-EGFR$_{K521}$, and α2-3,6,8,9 Neuraminidase A–digested Fc-EGFR and EGFR$_{K521}$. **B,** MALDI-TOF spectra of permethylated N-glycan pools from Fc-EGFR (lower and higher pH ranges protein species were separated in pool 1 and 2) and Fc-EGFR$_{K521}$. Monosaccharide symbols used were as follows: red triangle, fucose; blue square, *N*-acetylglucosamine; green circle, mannose; yellow circle, galactose; pink diamond, *N*-acetylneuraminic acid. **C,** Melting curves of Fc-EGFR and Fc-EGFR$_{K521}$. Molar ellipticity at 208 nm of a 0.2 g/L Fc-EGFR solution in 0.01 mol/L PBS was recorded from 23°C to 100°C in 1°C steps using a 1-mm pathlength cuvette. Melting curves are depicted as dotted lines and fitted curves as solid lines.

protein species, whereas the 2D pattern of the desialylated protein species of Fc-EGFR$_{K521}$ remained the same (Fig. 6A, fourth row). This suggested absence of sialylation in the EGFR$_{K521}$ variant. To definitively determine their glycosylation patterns, Fc-EGFR$_{K521}$ and Fc-EGFR proteins excised from 2D gels were digested with PNGase F. Released *N*-glycans were extracted from the gel,

permethylated, and finally analyzed by MALDI-TOF mass spectrometry. This analysis showed that the $EGFR_{K521}$ variant exhibits a clearly aberrant glycosylation pattern consisting of unsialylated mostly high-mannose *N*-glycans and complete absence of complex-type *N*-glycans (Fig. 6B).

$EGFR_{K521}$ is less stable compared with EGFR

As protein glycosylation and folding are coupled processes in the ER (32–35), glycosylation has a direct impact on protein stability (36–38). Therefore, we compared Fc-EGFR and Fc-$EGFR_{K521}$ proteins on the secondary structure level using far-UV CD spectroscopy. This analysis showed clear differences in secondary structure (Supplementary Fig. S5) and stability of Fc-EGFR and Fc-$EGFR_{K521}$ proteins with the Fc-EGFR protein being more stable and a delta in melting temperatures of >10°C (Tm Fc-$EGFR_{K521}$ = 60.63°C, Tm Fc-EGFR = 72.14°C, Fig. 6C). Together, the differential pattern of protein glycosylation and the reduced overall protein stability likely accounts for the affinity differences and the significantly reduced cetuximab activity in cells expressing this receptor variant.

CetuGEX overcomes $EGFR_{K521}$-mediated resistance

As attachment of cetuximab to $EGFR_{K521}$-expressing cells was still preserved, we reasoned that a next-generation EGFR antibody relying rather on cell-based effector mechanisms (e.g., ADCC) than on pathway inhibition could potentially overcome resistance in cells expressing the $EGFR_{K521}$ variant. To test this experimentally, we studied induction of ADCC using CetuGEX, an antibody with optimized Fc glycosylation targeting the same epitope with the same affinity as cetuximab (39). Because of the glyco-optimization (absence of core fucose and the presence of bisecting GlcNAc within the antibody Fc part) CetuGEX binds with higher affinity to the FcγRIIIA on human immune effector cells, thereby strongly enhancing its ADCC activity (40–42). As glyco-optimized antibodies may not be tested *in vivo* for ADCC due to impaired interaction with murine effector cell Fc receptors, we performed these experiments *in vitro* using ADCC assays in HNSCC cell lines. We chose two pairs of cell lines with highly similar EGFR membrane expression levels for ADCC comparisons between $EGFR_{K521}$ and EGFR. Both antibodies showed significant ADCC induction in the cell lines not expressing the K-allele (UT-SCC 14 and UT-SCC 42A), with CetuGEX being slightly but significantly more active than cetuximab (Fig. 7A). In the SAT and UT-SCC 5 cell lines with high K-allele frequency, much higher antibody concentrations of cetuximab were necessary for ADCC induction, reflecting both the reduced binding affinity of this interaction with the target and the more inefficient interaction with effector cells due to non-optimized Fc configuration (Fig. 7A). In contrast, CetuGEX was clearly more efficient in inducing ADCC in the SAT and UT-SCC 5 cell lines, suggesting that the slightly reduced binding affinity could be compensated by enhanced effector cell recruitment (Fig. 7A). As the susceptibility to NK-cell–mediated lysis can vary between different cell lines, ADCC assays with CetuGEX were performed also in Ba/F3 cells carrying either EGFR or $EGFR_{K521}$ (Fig. 7B). These experiments showed comparable efficacy of this antibody in cells with either of the receptor variants (Fig. 7B). These experiments were not informative for cetuximab treatment as the low EGFR membrane expression level precluded calculation of meaningful EC_{50} values (Supplementary Fig. S6).

These results indicate that sensitivity to EGFR targeting may be restored by using ADCC-optimized antibodies in $EGFR_{K521}$-expressing HNSCC.

Discussion

HNSCC is a prototype disease in which the addition of a molecularly targeted drug to chemotherapy has shown promise, but is still associated with a high rate of primary and acquired resistance. Personalized strategies have to be designed to tailor our expensive molecular drugs to the target population to ultimately optimize our cancer care.

In this study, we investigated a frequent SNP located at position 521 within the extracellular EGFR domain. As in previously published clinical series of HNSCC patients, our own patients expressing the K-allele showed shorter progression-free survival than those expressing only the R-allele when treated with cetuximab. This polymorphism involves a *prima vista* biochemically insignificant amino acid exchange from arginine to lysine and its distance from the cetuximab epitope theoretically suggests that it may not interfere with cetuximab binding. In line with this assumption, we found preserved cell attachment of cetuximab to $EGFR_{K521}$, however, with slightly reduced affinity compared with EGFR. However, this slight impairment resulted in a delicate inability of cetuximab to inhibit cell proliferation and EGFR pathway activation *in vitro* and *in vivo*. Interestingly, the single amino acid substitution of the $EGFR_{K521}$ variant resulted in drastic changes from complex-type to unsialylated high-mannose *N*-glycans, potentially accounting for reduced stability and cetuximab affinity (43). Comparison of the two EGFR variants in an HNSCC-independent Ba/F3 cellular model system suggested that (i) EGFR functionality was preserved in the $EGFR_{K521}$ variant and (ii) the EGFR itself (and not other molecular features hypothetically correlating with $EGFR_{K521}$ expression in HNSCC) mediates resistance. As only affinity, but not cellular attachment of cetuximab to $EGFR_{K521}$-expressing cells was impaired, we explored alternative targeting approaches with an antibody that relies less on pathway inhibition. To this end, we used the glyco-optimized CetuGEX antibody that binds with higher affinity to FcγRIIIA on human immune effector cells, thereby strongly enhancing its ADCC activity. This antibody restored sensitivity to EGFR targeting in HNSCC expressing the $EGFR_{K521}$ variant.

One important aspect of our work is the finding that EGFR functionality was preserved in the $EGFR_{K521}$ variant. As our cellular model exclusively depends on the EGFR pathway for survival, our ligand stimulation data demonstrating equal levels of pathway activation in both EGFR variants is highly informative. Moreover, this finding was somewhat expected as $EGFR_{K521}$ expression does not lead to any distinct phenotype in the general population. However, this finding is in contrast to a publication from 1994 reporting that EGFR pathway activation by TGFα, one of the EGFR ligands, was impaired in *$EGFR_{K521}$*-transduced CHO cells (44). To our knowledge, this was the only experimental evidence supporting the notion of dysfunctional EGFR pathway activation in the $EGFR_{K521}$ variant, which served as a reference for a large number of subsequent studies. This hypothesis is clearly challenged by the data presented in this article.

From a clinical perspective, our data is highly relevant as translation into the clinic may change current paradigms in terms of biomarker-driven patient selection for patients with

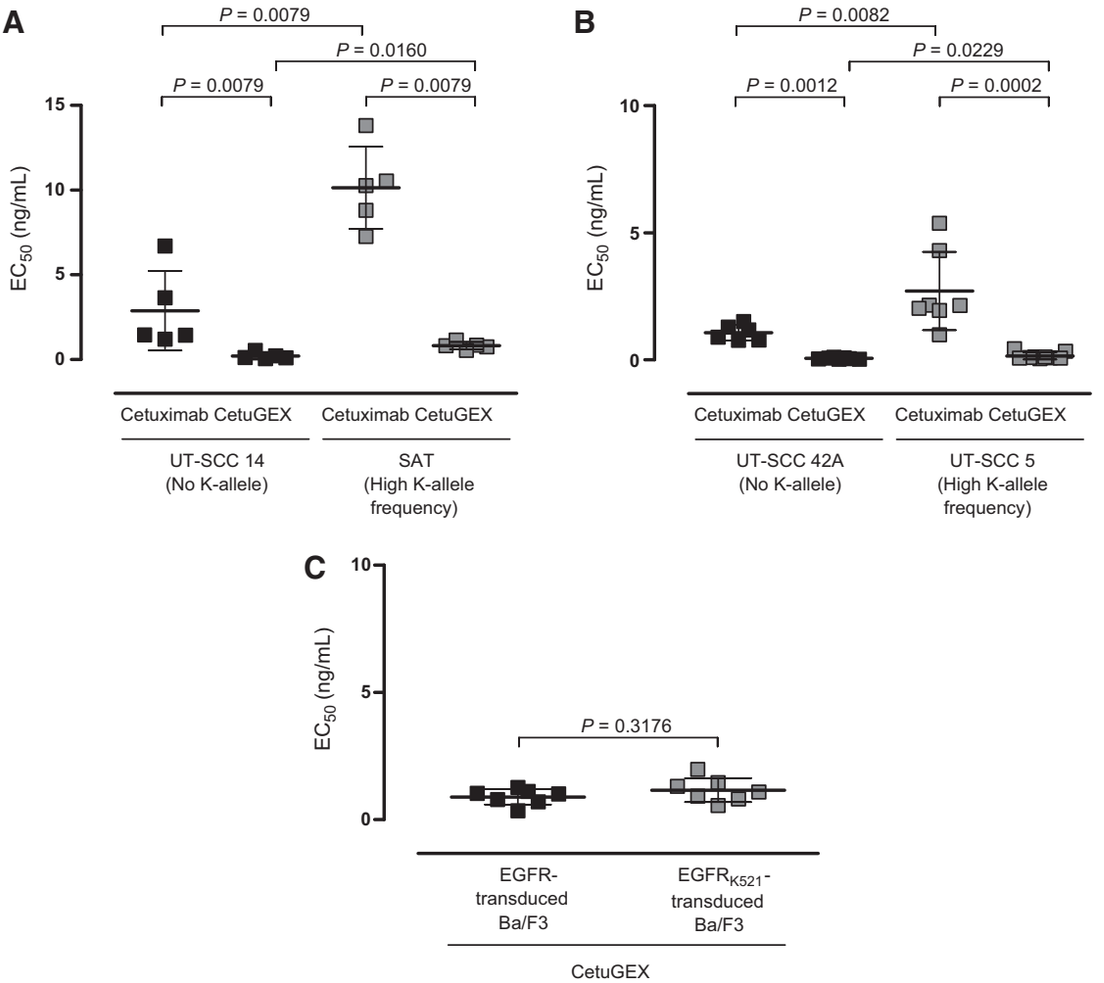

Figure 7.

ADCC induction in HNSCC cell lines with low and high K-allele frequency as well as EGFR-transduced Ba/F3 cells by cetuximab and CetuGEX. EC_{50} values of HNSCC cell lines with no and high K-allele frequency treated with cetuximab or CetuGEX (**A** and **B**) or EGFR/$EGFR_{K521}$ transduced Ba/F3 cell lines treated with CetuGEX (**C**). The europium release assay was performed with KHYG1-CD16aF as effector cell line. All datasets consist of 5–7 independent experiments ±SEM. *, $P < 0.05$; **, $P < 0.01$ by Mann–Whitney test (**A**) and Student *t* test (**B**). n.s., not significant.

HNSCC. As this EGFR polymorphism is expressed in more than 40% of individuals, it has been previously studied in clinical cohorts. A recent meta-analysis confirmed that this polymorphism is not associated with the risk of cancer (25). In HNSCC patients, there seems to be a favorable prognostic role of the $EGFR_{K521}$ variant in patients that do not receive EGFR-targeted agents (45). Two retrospective HNSCC series were reported on its predictive potential in the context of EGFR-targeted therapy. One of these studies observed a trend towards a higher risk of tumor progression ($n = 51$) (24), the other one reduced overall survival in patients expressing the $EGFR_{K521}$ variant ($n = 45$; ref. 22) undergoing cetuximab-containing therapy. Our own clinical cohort ideally complements these previous findings and our clear-cut preclinical data reveal for the first time the molecular basis for cetuximab resistance in this setting. In view of this, larger prospective clinical trials are clearly needed to confirm the predictive value of this potential biomarker in HNSCC, to determine the most discriminative allele burden cutoff predicting lack of response as well as to evaluate alternative options to overcome resistance. As simple dose escalation of cetuximab to compensate for reduced affinity is difficult in patients for toxicity reasons, future studies involving novel EGFR antibody–targeting approaches are therefore clearly warranted. These may include cytotoxicity engineered EGFR antibodies (e.g., CetuGEX; refs. 46, 47) but potentially also other strategies, such as affinity-optimized EGFR antibodies (48), EGFR targeting mono- or biparatopic nanobodies with better tissue penetration (49, 50), or EGFR antibodies with different epitope fine specificity (51).

Moreover, preclinical and clinical studies should also address this polymorphism's role as a potential predictor of cetuximab sensitivity in RAS wild-type colorectal cancer. To date, the available clinical data are inconclusive in this setting, presumably due to more heterogeneous chemotherapy backbones and

potential confounders with its prognostic role (52–54). Although our data were partly generated in HNSCC-independent models, this may not necessarily permit to translate these findings to the colon cancer context. This is because, among other issues, the antibody affinity required for pathway inhibition may differ in these cancer entities.

Taken together, our results strongly support preliminary clinical evidence for insensitivity of head and neck tumor cells expressing $EGFR_{K521}$ to cetuximab. This polymorphism may allow to identify a substantial proportion of patients not likely to derive benefit from this common and relatively expensive EGFR-directed therapeutic strategy by a genomic test. Moreover, such patients should be offered alternative EGFR-targeted approaches in prospective clinical trials to ultimately confirm the validity of this concept in the clinical setting.

Disclosure of Potential Conflicts of Interest

S. Laban is a consultant/advisory board member for AstraZeneca. S. Goletz is a chief executive officer/chief scientific officer at Glycotope GmbH. R. Knecht is a consultant/advisory board member for Head and Neck Oncology. No potential conflicts of interest were disclosed by the other authors.

Authors' Contributions

Conception and design: F. Braig, V. Blanchard, S. Goletz, C. Bokemeyer, M. Binder

Development of methodology: F. Braig, M. Kriegs, B. Habel, I.B. Batalla, B. Fehse, S. Loges, M. Binder

Acquisition of data (provided animals, acquired and managed patients, provided facilities, etc.): F. Braig, M. Kriegs, B. Habel, T. Grob, M. Voigtlaender, K. Biskup, M. Sack, A. Thalhammer, I.B. Batalla, S. Laban, A. Danielczyk, E. Jakubowicz, B. Märkl, M. Trepel, R. Knecht, K. Riecken, S. Loges, C. Bokemeyer, M. Binder

Analysis and interpretation of data (e.g., statistical analysis, biostatistics, computational analysis): F. Braig, M. Kriegs, B. Habel, M. Voigtlaender, K. Biskup, V. Blanchard, M. Sack, A. Thalhammer, I.B. Batalla, S. Laban, A. Danielczyk, M. Trepel, S. Loges, M. Binder

Writing, review, and/or revision of the manuscript: F. Braig, B. Habel, T. Grob, M. Voigtlaender, K. Biskup, V. Blanchard, M. Sack, I.B. Batalla, S. Laban, A. Danielczyk, S. Goletz, E. Jakubowicz, B. Märkl, R. Knecht, K. Riecken, B. Fehse, S. Loges, C. Bokemeyer, M. Binder

Administrative, technical, or material support (i.e., reporting or organizing data, constructing databases): F. Braig, I. Braren, E. Jakubowicz, B. Märkl, M. Trepel

Study supervision: F. Braig, V. Blanchard, M. Binder

Other (histologic confirmation of tumor material): E. Jakubowicz, B. Märkl

Acknowledgments

The authors thank Anita Schulenkorf, Konstantin Hoffer, Steffi Sawall, Monja Paasche, Sina Metz, and Franziska Axt for expert technical assistance.

Grant Support

This work was supported by the "Deutsche Forschungsgemeinschaft" (grant BI 1711/1 to M. Binder).

The costs of publication of this article were defrayed in part by the payment of page charges. This article must therefore be hereby marked *advertisement* in accordance with 18 U.S.C. Section 1734 solely to indicate this fact.

Received March 16, 2016; revised October 24, 2016; accepted November 13, 2016; published OnlineFirst December 28, 2016.

References

1. Siegel R, Naishadham D, Jemal A. Cancer statistics, 2012. CA Cancer J Clin 2012;62:10–29.
2. Budach V, Cho C-H, Sedlmaier B, Wittlinger M, Iro H, Engenhart-Cabillic R, et al. Five years' results of the German ARO 04-01 trial of concurrent 72 Gy hyperfractionated accelerated radiation therapy (HART) plus once weekly cisplatinum/5-FU versus mitomycin C/5-FU in stage IV head and neck cancer. ASCO Annual Meeting 2012 (abstr. 5512).
3. Bonner JA, Harari PM, Giralt J, Cohen RB, Jones CU, Sur RK, et al. Radiotherapy plus cetuximab for locoregionally advanced head and neck cancer: 5-year survival data from a phase 3 randomised trial, and relation between cetuximab-induced rash and survival. Lancet Oncol 2010;11:21–8.
4. Forastiere AA, Zhang Q, Weber RS, Maor MH, Goepfert H, Pajak TF, et al. Long-term results of RTOG 91-11: a comparison of three nonsurgical treatment strategies to preserve the larynx in patients with locally advanced larynx cancer. J Clin Oncol 2013; 31:845–52.
5. Posner MR, Hershock DM, Blajman CR, Mickiewicz E, Winquist E, Gorbounova V, et al. Cisplatin and fluorouracil alone or with docetaxel in head and neck cancer. N Engl J Med 2007;357:1705–15.
6. Vermorken JB, Remenar E, van Herpen C, Gorlia T, Mesia R, Degardin M, et al. Cisplatin, fluorouracil, and docetaxel in unresectable head and neck cancer. N Engl J Med 2007;357:1695–704.
7. Vermorken JB, Mesia R, Rivera F, Remenar E, Kawecki A, Rottey S, et al. Platinum-based chemotherapy plus cetuximab in head and neck cancer. N Engl J Med 2008;359:1116–27.
8. Vermorken JB, Stohlmacher-Williams J, Davidenko I, Licitra L, Winquist E, Villanueva C, et al. Cisplatin and fluorouracil with or without panitumumab in patients with recurrent or metastatic squamous-cell carcinoma of the head and neck (SPECTRUM): an open-label phase 3 randomised trial. Lancet Oncol 2013;14:697–710.
9. Vermorken JB, Trigo J, Hitt R, Koralewski P, Diaz-Rubio E, Rolland F, et al. Open-label, uncontrolled, multicenter phase II study to evaluate the efficacy and toxicity of cetuximab as a single agent in patients with recurrent and/or metastatic squamous cell carcinoma of the head and neck who failed to respond to platinum-based therapy. J Clin Oncol 2007;25:2171–7.
10. Di Nicolantonio F, Martini M, Molinari F, Sartore-Bianchi A, Arena S, Saletti P, et al. Wild-type BRAF is required for response to panitumumab or cetuximab in metastatic colorectal cancer. J Clin Oncol 2008;26: 5705–12.
11. Lievre A, Bachet JB, Le Corre D, Boige V, Landi B, Emile JF, et al. KRAS mutation status is predictive of response to cetuximab therapy in colorectal cancer. Cancer Res 2006;66:3992–5.
12. Lievre A, Laurent-Puig P. Genetics: predictive value of KRAS mutations in chemoresistant CRC. Nat Rev Clin Oncol 2009;6:306–7.
13. Wheeler DL, Dunn EF, Harari PM. Understanding resistance to EGFR inhibitors-impact on future treatment strategies. Nat Rev Clin Oncol 2010;7:493–507.
14. Licitra L, Storkel S, Kerr KM, Van Cutsem E, Pirker R, Hirsch FR, et al. Predictive value of epidermal growth factor receptor expression for first-line chemotherapy plus cetuximab in patients with head and neck and colorectal cancer: analysis of data from the EXTREME and CRYSTAL studies. Eur J Cancer 2013;49:1161–8.
15. Wheeler SE, Suzuki S, Thomas SM, Sen M, Leeman-Neill RJ, Chiosea SI, et al. Epidermal growth factor receptor variant III mediates head and neck cancer cell invasion via STAT3 activation. Oncogene 2010;29:5135–45.
16. Sok JC, Coppelli FM, Thomas SM, Lango MN, Xi S, Hunt JL, et al. Mutant epidermal growth factor receptor (EGFRvIII) contributes to head and neck cancer growth and resistance to EGFR targeting. Clin Cancer Res 2006; 12:5064–73.
17. Liao HW, Hsu JM, Xia W, Wang HL, Wang YN, Chang WC, et al. PRMT1-mediated methylation of the EGF receptor regulates signaling and cetuximab response. J Clin Invest 2015;125:4529–43.
18. Brand TM, Iida M, Stein AP, Corrigan KL, Braverman CM, Luthar N, et al. AXL mediates resistance to cetuximab therapy. Cancer Res 2014;74: 5152–64.
19. Rampias T, Giagini A, Siolos S, Matsuzaki H, Sasaki C, Scorilas A, et al. RAS/PI3K crosstalk and cetuximab resistance in head and neck squamous cell carcinoma. Clin Cancer Res 2014;20:2933–46.

20. Stransky N, Egloff AM, Tward AD, Kostic AD, Cibulskis K, Sivachenko A, et al. The mutational landscape of head and neck squamous cell carcinoma. Science 2011;333:1157–60.
21. Krohn V, Wiegand S, Werner JA, Mandic R. EGFR codon 497 polymorphism - implications for receptor sensitivity to inhibitors in HNSCC cell lines. Anticancer Res 2011;31:59–65.
22. Stoehlmacher-Williams J, Obermann L, Ehninger G, Goekkurt E. Polymorphisms of the epidermal growth factor receptor (EGFR) and survival in patients with advanced cancer of the head and neck (HNSCC). Anticancer Res 2012;32:421–5.
23. Langer CJ. Exploring biomarkers in head and neck cancer. Cancer 2012;118:3882–92.
24. Klinghammer K, Knodler M, Schmittel A, Budach V, Keilholz U, Tinhofer I. Association of epidermal growth factor receptor polymorphism, skin toxicity, and outcome in patients with squamous cell carcinoma of the head and neck receiving cetuximab-docetaxel treatment. Clin Cancer Res 2010;16:304–10.
25. Wang Y, Zha L, Liao D, Li X. A meta-analysis on the relations between EGFR R521K polymorphism and risk of cancer. Int J Genomics 2014;2014: 312102.
26. Braig F, Marz M, Schieferdecker A, Schulte A, Voigt M, Stein A, et al. Epidermal growth factor receptor mutation mediates cross-resistance to panitumumab and cetuximab in gastrointestinal cancer. Oncotarget 2015;6:12035–47.
27. Weber K, Bartsch U, Stocking C, Fehse B. A multicolor panel of novel lentiviral "gene ontology" (LeGO) vectors for functional gene analysis. Mol Ther 2008;16:698–706.
28. Weber K, Mock U, Petrowitz B, Bartsch U, Fehse B. Lentiviral gene ontology (LeGO) vectors equipped with novel drug-selectable fluorescent proteins: new building blocks for cell marking and multi-gene analysis. Gene Ther 2010;17:511–20.
29. Blank K, Lindner P, Diefenbach B, Pluckthun A. Self-immobilizing recombinant antibody fragments for immunoaffinity chromatography: generic, parallel, and scalable protein purification. Protein Expr Purif 2002;24:313–22.
30. Wedepohl S, Kaup M, Riese SB, Berger M, Dernedde J, Tauber R, et al. N-glycan analysis of recombinant L-Selectin reveals sulfated GalNAc and GalNAc-GalNAc motifs. J Proteome Res 2010;9:3403–11.
31. Hanash SM, Pitteri SJ, Faca VM. Mining the plasma proteome for cancer biomarkers. Nature 2008;452:571–9.
32. Hoffmann D, Flörke H. A structural role for glycosylation: lessons from the hp model. Fold Des 1998;3:337–43.
33. Parodi AJ. Protein glucosylation and its role in protein folding. Annu Rev Biochem 2000;69:69–93.
34. Parodi AJ. Role of N-oligosaccharide endoplasmic reticulum processing reactions in glycoprotein folding and degradation. Biochem J 2000; 348:1–13.
35. Live DH, Kumar RA, Beebe X, Danishefsky SJ. Conformational influences of glycosylation of a peptide: a possible model for the effect of glycosylation on the rate of protein folding. Proc Natl Acad Sci 1996;93:12759–61.
36. Bishayee S. Role of conformational alteration in the epidermal growth factor receptor (EGFR) function. Biochem Pharmacol 2000;60:1217–23.
37. Petrescu A-J, Milac A-L, Petrescu SM, Dwek RA, Wormald MR. Statistical analysis of the protein environment of N-glycosylation sites: implications for occupancy, structure, and folding. Glycobiology 2004;14:103–14.
38. Shental-Bechor D, Levy Y. Effect of glycosylation on protein folding: A close look at thermodynamic stabilization. Proc Natl Acad Sci 2008; 105:8256–61.
39. Fiedler W, Sessa C, Gianni L, Cresta S, Schulze-Bergkamen H, Weidmann J, et al. First-in-human phase I study of CetuGEX, a novel anti-EGFR monoclonal antibody (mAb) with optimized glycosylation and antibody dependent cellular cytotoxicity. J Clin Oncol 31, 2013 (suppl; abstr 3008).
40. Shields RL, Lai J, Keck R, O'Connell LY, Hong K, Meng YG, et al. Lack of fucose on human IgG1 N-linked oligosaccharide improves binding to human Fcgamma RIII and antibody-dependent cellular toxicity. J Biol Chem 2002;277:26733–40.
41. Shinkawa T, Nakamura K, Yamane N, Shoji-Hosaka E, Kanda Y, Sakurada M, et al. The absence of fucose but not the presence of galactose or bisecting N-acetylglucosamine of human IgG1 complex-type oligosaccharides shows the critical role of enhancing antibody-dependent cellular cytotoxicity. J Biol Chem 2003;278:3466–73.
42. Suzuki E, Niwa R, Saji S, Muta M, Hirose M, Iida S, et al. A nonfucosylated anti-HER2 antibody augments antibody-dependent cellular cytotoxicity in breast cancer patients. Clin Cancer Res 2007;13:1875–82.
43. Rudd PM, Elliott T, Cresswell P, Wilson IA, Dwek RA. Glycosylation and the immune system. Science 2001;291:2370–6.
44. Moriai T, Kobrin MS, Hope C, Speck L, Korc M. A variant epidermal growth factor receptor exhibits altered type alpha transforming growth factor binding and transmembrane signaling. Proc Natl Acad Sci U S A 1994; 91:10217–21.
45. Su NW, Leu YS, Lee JC, Liu CJ, Cheng CY, Lin JS, et al. EGF and EGFR genetic polymorphisms predict prognosis in locally advanced pharyngolaryngeal squamous cell carcinoma patients receiving postoperative concurrent chemoradiotherapy. Onco Targets Ther 2014;7:2197–204.
46. Derer S, Cossham M, Rosner T, Kellner C, Beurskens FJ, Schwanbeck R, et al. A complement-optimized EGFR antibody improves cytotoxic functions of polymorphonuclear cells against tumor cells. J Immunol 2015;195:5077–87.
47. Lohse S, Meyer S, Meulenbroek LA, Jansen JH, Nederend M, Kretschmer A, et al. An anti-EGFR IgA that displays improved pharmacokinetics and myeloid effector cell engagement in vivo. Cancer Res 2016;76:403–17.
48. Lippow SM, Wittrup KD, Tidor B. Computational design of antibody-affinity improvement beyond in vivo maturation. Nat Biotechnol 2007; 25:1171–6.
49. Roovers RC, Laeremans T, Huang L, De Taeye S, Verkleij AJ, Revets H, et al. Efficient inhibition of EGFR signaling and of tumour growth by antagonistic anti-EFGR Nanobodies. Cancer Immunol Immunother 2007;56: 303–17.
50. Roovers RC, Vosjan MJ, Laeremans T, el Khoulati R, de Bruin RC, Ferguson KM, et al. A biparatopic anti-EGFR nanobody efficiently inhibits solid tumour growth. Int J Cancer 2011;129:2013–24.
51. Machiels JP, Specenier P, Krauss J, Dietz A, Kaminsky MC, Lalami Y, et al. A proof of concept trial of the anti-EGFR antibody mixture Sym004 in patients with squamous cell carcinoma of the head and neck. Cancer Chemother Pharmacol 2015;76:13–20.
52. Goncalves A, Esteyries S, Taylor-Smedra B, Lagarde A, Ayadi M, Monges G, et al. A polymorphism of EGFR extracellular domain is associated with progression free-survival in metastatic colorectal cancer patients receiving cetuximab-based treatment. BMC Cancer 2008;8:169.
53. Press OA, Zhang W, Gordon MA, Yang D, Lurje G, Iqbal S, et al. Gender-related survival differences associated with EGFR polymorphisms in metastatic colon cancer. Cancer Res 2008;68:3037–42.
54. Hsieh YY, Tzeng CH, Chen MH, Chen PM, Wang WS. Epidermal growth factor receptor R521K polymorphism shows favorable outcomes in KRAS wild-type colorectal cancer patients treated with cetuximab-based chemotherapy. Cancer Sci 2012;103:791–6.